Zuschriften

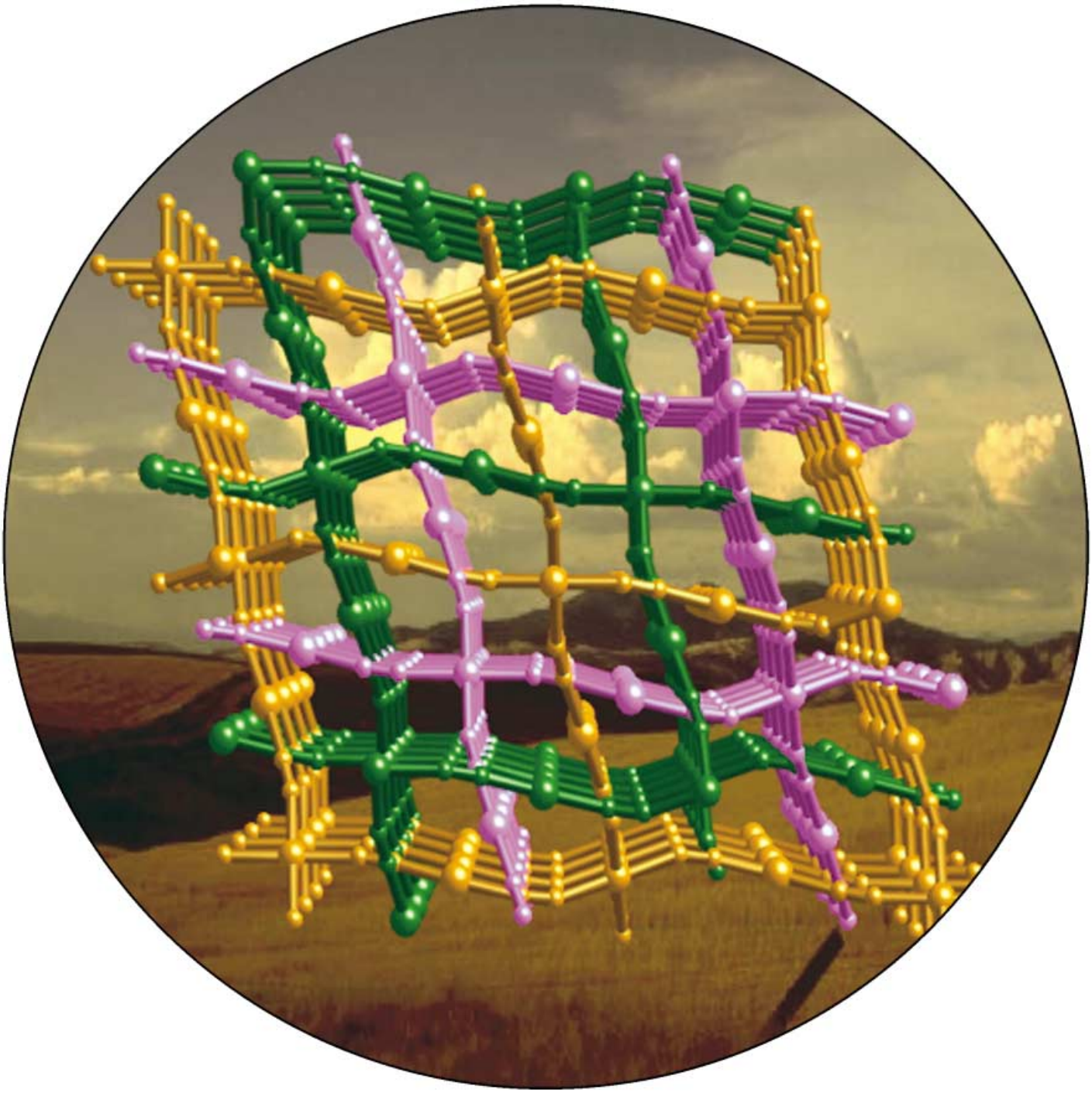

Die drei unabhängigen, verzahnten dreidimensionalen Netze in $[Fe(pdm)(H_2O)\{Ag(CN)_2\}_2]\cdot H_20$ bilden nach Verlust koordinierter Wassermoleküle ein zusammenhängendes dreidimensionales Netz. Diese reversible Umwandlung führt zu drastischen Änderungen bei den Spin-Crossover-Übergängen. Weitere Informationen dazu gibt die Zuschrift von J. A. Real und Mitarbeitern auf den folgenden Seiten.

DOI: 10.1002/ange.200351853

Hysteresis in Fe-CN-Ag/Au Networks

Crystalline-State Reaction with Allosteric Effect in Spin-Crossover, Interpenetrated Networks with Magnetic and Optical Bistability**

*Virginie Niel, Amber L. Thompson, M. Carmen Muñoz, Ana Galet, Andrés E. Goeta, and José A. Real**

The versatility of metal–organic chemistry offers a unique opportunity to construct multifunctional materials based on the assembly of molecular building blocks. Such an approach can lead to the design of coordination polymers with specific network topologies and potentially interesting properties.[1] Incorporation of iron(II) spin crossover (SCO) building blocks in such framework structures is particularly suitable for these purposes as the labile electronic configurations of the iron units may be switched between the high- (HS) and low-spin (LS) states. This switching leads to distinctive changes in magnetism, color, and structure, which may be induced by variation of temperature and/or pressure and by light irradiation.[2] Strong signal generation and hysteresis (memory effect) may be achieved when rigid linkers, which allow communication between the SCO centers, propagate the structural changes cooperatively to the whole framework conferring a bistable character to the material.[3–5] The construction of sensory and memory devices is the ultimate goal.

Hofmann-like open frame coordination polymers have been the subject of much research for many years.[6] Nevertheless, incorporation of iron(II) SCO building blocks in such systems is relatively recent.[7] Following this strategy we have shown the suitability of cyano-metallate complexes as connectors between iron(II) SCO centers to build highly cooperative thermo-, piezo-, and photo-switchable two- and three-dimensional coordination polymers.[8–10] A further important aspect for developing multifunctional materials based on these polymers stems from their porous nature,[11] which opens opportunities for investigating the interplay between inclusion chemistry and SCO signal generation.[12,13] Herein we report on the incorporation of electronic SCO, molecular recognition, and crystalline-state reaction[14] switching events and their cooperative interactions in [Fe(pmd)-$(H_2O)\{M(CN)_2\}_2]\cdot H_2O$ (**1**) (pmd = pyrimidine; M = Ag (**1Ag**) or Au (**1Au**)). This is a cyanide-based bimetallic coordination polymer made up of triple interpenetrated, 4-connected, three-dimensional, open-frame networks.

Compound **1** is monoclinic (space group $P2_1/c$) whatever the spin state (the structural parameters reported below correspond to the HS state).[15] Two distinct iron atoms, Fe(1) and Fe(2) (see Figure 2), which define the inversion center of an elongated $\{Fe(1)N_6\}$ and a compressed $\{Fe(2)N_4O_2\}$ coordination octahedron, respectively, constitute the building blocks of the structure. The four equatorial positions are occupied by the cyanide nitrogen atoms of the $[M(CN)_2]^-$ groups while the apical positions are occupied by two nitrogen atoms of two pmd ligands (Fe(1)) and by two water molecules (Fe(2)). The $[M(CN)_2]^-$ groups link the Fe(1) and Fe(2) atoms generating {Fe(1)-NC-M(1)-CN-Fe(2)-NC-M(2)-CN-} groups which connect to form rectangular motifs. These rectangles have edges Fe(1)···Fe(1) = 20.5775(7) (**1Ag**), 20.3860(6) Å (**1Au**) and Fe(1)···Fe(2) = 10.6417(2) (**1Ag**), 10.5643(2) Å (**1Au**). The edge sharing rectangles define an infinite set of parallel layers pillared by $[M(CN)_2]^-$ groups. The resulting 4-connected 3D network corresponds to the expanded version of the prototypical $CdSO_4$ net decorated by the coordinating water molecules and the pmd ligands (Figure 1a).[16,17] The much larger intraframework spaces are occupied by two other identical but independent networks, which interpenetrate the first network and each other (Figure 1b). Communication between the three covalently bonded nets is through weaker metallophilic M···M interactions (average Ag···Ag and Au···Au distances 3.1813(3) and 3.2901(4) Å, respectively) and hydrogen bonds between the coordinated water molecules and the uncoordinated nitrogen atom of the pmd ligands (N(pmd)···H_20 = 2.805(3) Å (**1Ag**) and 2.762(6) Å (**1Au**); (Figure 2a, b). This arrangement accounts for the close proximity of the Fe(2) atom and the uncoordinated nitrogen atom, Fe(2)-OH_2···N(pmd), which provides favorable conditions for a topochemical reaction to take place (Figure 2a).

Complete and rapid loss of both ligated and nonbonded water molecules occurs simultaneously in the temperature range 345–399 K (**1Ag**) and 323–382 K (**1Au**). X-ray powder diffraction spectra (XRPD) were recorded on **1Au** at 290 K and 373 K at ambient pressure and at 290 K under vacuum. The data obtained clearly confirms that at 290 K at ambient pressure the sample is in the hydrated state, in agreement with results obtained from single-crystal measurements. The X-ray spectra taken at 373 K at ambient pressure and at 290 K under vacuum are essentially identical though different to the spectra of the hydrated sample, thus revealing the structural changes caused by the loss of the water molecules. Ab initio indexing of the powder pattern of the dehydrated sample clearly shows the massive cell-contraction (ca. 2.5 Å) taking place along the *a* axis, previously assumed from the observed shift of the 200 reflection from 12.3(2)° to 14.5(2)° (Supporting Information). This large and reversible structural modification involving not only the loss of an unbound water

[*] Prof. Dr. J. A. Real, Dr. V. Niel
Institut de Ciencia Molecular/Departament de Química Inorgànica
Universitat de València
Doctor Moliner 50, 46100 Burjassot, València (Spain)
Fax: (+34) 96-386-4322
E-mail: jose.a.real@uv.es
A. L. Thompson, Dr. A. E. Goeta
Department of Chemistry
University of Durham
South Road, Durham, DH1 3LE (UK)
Prof. Dr. M. C. Muñoz, A. Galet
Departament de Física Aplicada
Universitat Politécnica de València
Camino de Vera s/n, 46071 València (Spain)

[**] We are grateful for financial assistance from the Ministerio Español de Ciencia y Tecnología (project BQU 2001–2928), The Royal Society for a Study Visit and a Join Project awards. ALT thanks EPSRC for a Postgraduate Fellowship. AG thanks to the Universitat Politècnica de València for a predoctoral fellowship.

Supporting information for this article is available on the WWW under http://www.angewandte.org or from the author.

  DOI: 10.1002/ange.200351853

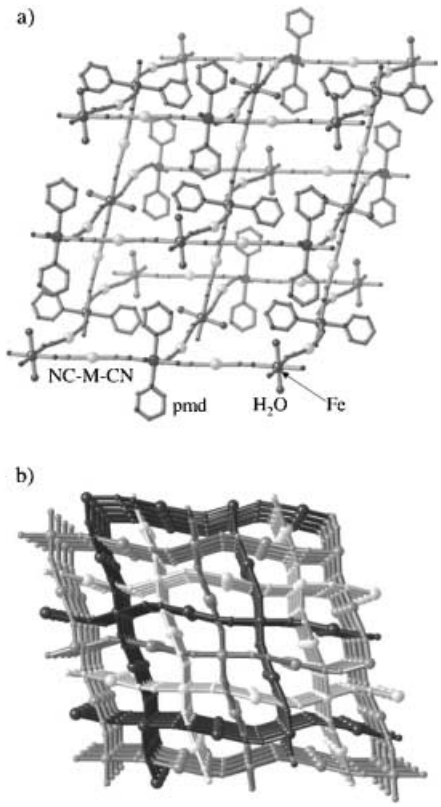

Figure 1. a) Fragment of the 3D network of **1** displaying the expanded version of the $CdSO_4$ structure. b) Perspective view of the three interlocked networks.

molecule but more importantly the loss of a coordinating water molecule, affects the integrity of the single crystals of **2** (they crack and become effectively a polycrystalline powder) precluding the in situ structure determination from single-crystal diffraction techniques. The structure determination of **2Au** was then carried out from a rigid-body Rietveld refinement of the hydrated model, excluding the water molecules, using the newly determined cell parameters.[18] No change in space group has been observed following the **1**↔**2** transformation. There are two crystallographically distinct $\{FeN_6\}$ distorted octahedrons in **2** whose Fe(1) and Fe(2) sites can be unambiguously identified with those corresponding to **1**. However, in contrast to **1**, the pmd ligand now bridges directly the Fe(1) and Fe(2) atoms defining a system of infinite chains {-Fe(1)-pmd-Fe(2)} running parallel to the *a* axis (Fe(1)···Fe(2) = 6.1927(4) Å) in **2**. The $[M(CN)_2]^-$ groups of one chain link with the equatorial positions of the iron centers, connecting adjacent chains and defining a single 3D network (Figure 2c, d). These significant structural changes are a consequence of the cooperative topochemical ligand substitution, which involves the concerted loss of the bonded water generating double coordination unsaturation at the Fe(2) centers and the coordination of the uncoordinated pmd nitrogen atom belonging to adjacent networks. A first example of topochemical conversion of a hydrogen-bonded into a covalent bonded supramolecular network was described for the binuclear $[\{Zn(sala)(H_2O)_2\}_2]\cdot 2H_2O$ compound (H_2sala = *N*-(2-hydroxybenzyl)-L-alanine), but this process was irreversible.[19] In contrast, when **1Au** and **1Ag** are exposed to an atmosphere of H_2O, selective absorption of this vapor induces the inverse reaction at the Fe(2) sites, regenerating the three independent 3D networks (Figure 2c, d). The system does not suffer any noticeable fatigue after repeating several **1**↔**2** cycles.

X-ray powder diffraction spectra of **1Ag** have also been recorded and it can be clearly observed that the behavior is similar to that described for the **1Au** compound. In spite of this, there are clear differences between **2Ag** and **2Au**, which point to either a different unit cell or a loss of symmetry from monoclinic to triclinic in **2Ag**. Further work is in progress to establish the cell parameters and space group for **2Ag**, with the aim of solving its crystal and molecular structure.

Figure 3 shows the temperature dependence of the $\chi_M T$ product for **1Ag** and **1Au**, χ_M being the molar magnetic susceptibility and T the temperature. At room temperature,

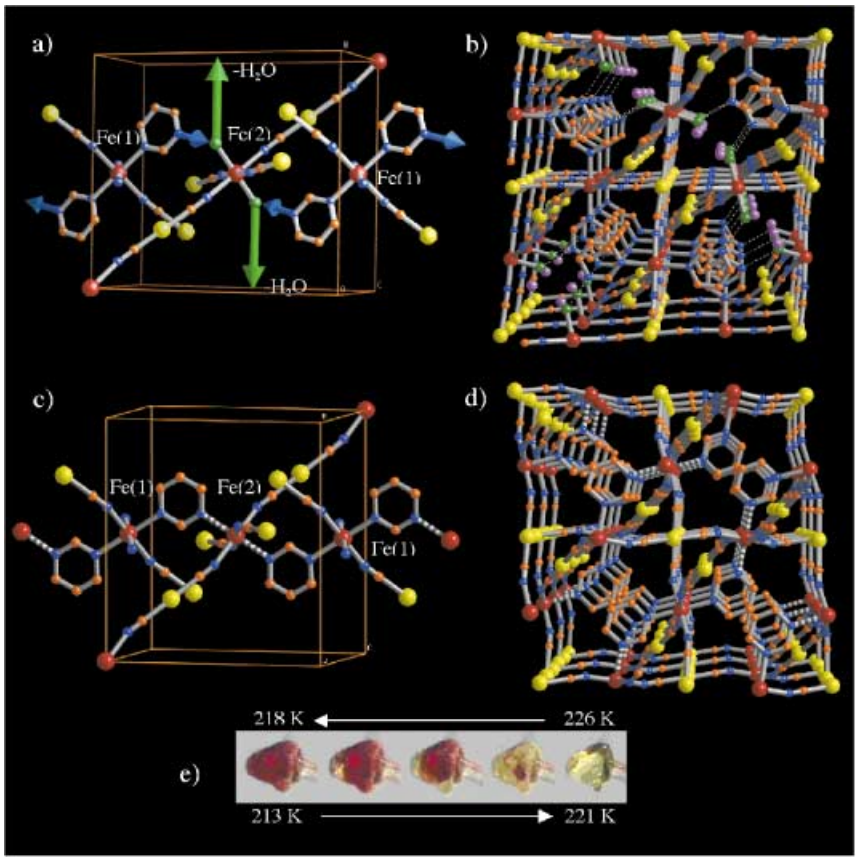

Figure 2. a) Unit cell of **1** showing fragments of three networks. Arrows on the uncoordinated nitrogen atoms (blue) and coordinated water molecules (green) indicate the dynamic event, which takes place during the topochemical solid-state reaction. b) Perspective view, [001], of the three nets showing the N(pmd)···H_2O hydrogen-bond system. c) Unit cell of **2Au** displaying the infinite chains defined by the bridging mode of the pmd ligand (striped bonds represent the new coordination bonds generated after dehydration. d) Perspective view of the new 3D network **2Au**. e) Photographs showing the color change of a **1Ag** single crystal around the critical region (yellow and deep red colors correspond to the high- and low-spin states, respectively).

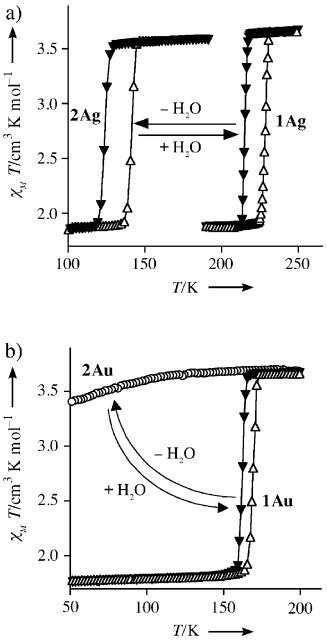

Figure 3. Magnetic susceptibility measurements displaying the first-order spin transition for a) **1Ag/2Ag** and b) **1Au/2Au**.

$\chi_M T$ is 3.7 for **1Ag** and 3.6 $cm^3 K mol^{-1}$ for **1Au**. These values are consistent with the iron(II) ion in the HS state. Upon cooling, $\chi_M T$ remains almost constant up to 218 K (**1Ag**) and 165 K (**1Au**), below these temperatures the $\chi_M T$ value undergoes a sharp decrease that is characteristic of a first order SCO transition. The $\chi_M T$ value drops to 1.8 (**1Ag**) and 1.7 (**1Au**) $cm^3 K mol^{-1}$ at 213 K and 159 K, respectively. The warming mode reveals the occurrence of thermal hysteresis. The critical temperatures for the cooling (T_c^{down}) and warming (T_c^{up}) modes (215 and 223 K (**1Ag**) and 163 and 171 K (**1Au**) respectively), indicate the occurrence of approximately 8 K wide hysteresis loops. At temperatures below T_c, the $\chi_M T$ value indicates that 50% of the iron(II) ions remains in the HS state for both compounds. As expected from their coordination environments, Fe(1) undergoes the HS↔LS transition while Fe(2) remains HS, which is in agreement with the structural data obtained at 120 K for both derivatives.

The temperature dependence of $\chi_M T$ was measured for the dehydrated **2Ag** and **2Au** forms (Figure 3a,b).For **2Ag** $\chi_M T$ is 3.6 $cm^3 K mol^{-1}$ at room temperature and remains constant down to 125 K, which indicates that the iron(II) ion is in the HS state in **2Ag**. The subsequent sharp decrease of $\chi_M T$ to a value of 1.9 $cm^3 K mol^{-1}$ is due to the occurrence of a spin transition. The warming mode reveals the occurrence of a 17 K wide thermal hysteresis loop. The critical temperatures are $T_c^{down} = 124$ K and $T_c^{up} = 141$ K. Compound **2Ag** has a hysteresis loop twice the width of **1Ag**, which denotes the expected increase of cooperativity when replacing the hydrogen-bonding internetwork interactions in **1** by stronger coordination bonds in the more rigid framework **2**. Compound **2Au** does not undergo a spin transition in the whole temperature range ($\chi_M T$ has a constant value of around 3.8 $cm^3 K mol^{-1}$ between room temperature and 120 K). This difference in the behavior of **2Ag** and **2Au** may be supported by the differences in the diffraction patterns observed for each of the compounds upon dehydration, see above. The marked down shift of T_c in **2Ag** and disappearance of SCO in **2Au** indicate a decrease of the ligand-field strength at the Fe(1) site and may be ascribed to the bridging mode of the pmd ligand. Recovery of the original SCO behavior of **1Ag** and **1Au** occurs when **2Ag** and **2Au** are left in air atmosphere.

Compounds **1Ag**, **1Au**, and **2Ag** undergo a dramatic change of color from pale yellow (HS state) to deep red (LS state) accompanying the SCO (Figure 2e). This thermochromic effect, observed in other 2D and 3D Fe^{II}–M^{II} (M = Ni, Pd, Pt) Hofmann-like SCO compounds, is a consequence of the increase in intensity of the metal-to-ligand charge transfer (MLCT) band around 550 nm, associated with the electron delocalization from the t_{2g} orbitals of the iron(II) ion to the π* orbitals of the ligands which is enhanced by the HS→LS spin change.[8]

In summary, the coordination polymers **1Au** and **1Ag** undergo thermally induced first-order, spin-crossover transitions with magnetic and chromatic bistability. They also participate in a controlled and fully reversible crystalline-state ligand substitution, involving coordination/uncoordination of gaseous water and pmd. This induces expansion/contraction of the nanoporous framework and the repeated allosteric transformation of the three interpenetrated nets into a single three-dimensional net (**2Ag** and **2Au**) without affecting their crystallinity but altering their SCO behavior significantly. Such a cooperative combination, in the same lattice, of different molecular events, such as recognition, allosterism, and electronic bistability is of fundamental significance for the generation of new switchable, multi-property materials.

Experimental Section

1Ag: was synthesized by slow diffusion, under an argon atmosphere, of two aqueous solutions containing stoichiometric amounts of $Fe(BF_4)_2 \cdot 6H_2O$ (0.185 mmol, 2 mL)/pyrimidine (0.374 mmol, 2 mL) in one side and $K[Ag(CN)_2]$ (0.374 mmol, 2 mL) in the other side of an H-shaped vessel. Pale yellow prismatic crystals were separated three weeks later. Yield approximately 50%. Elemental analysis (%) calcd for $C_8H_8N_6Ag_2O_2Fe$: C 19.54, H 1.61, N 17.09; found: C 20.05, H 1.98, N 16.76.

1Au: to an aqueous solution containing $FeCl_2$ (0.087 mmol, 4 mL) and pyrimidine (0.173 mmol, 4 mL) was added a water solution of $K[Au(CN)_2]$ (0.173 mmol, 6 mL). The resulting solution was stirred for 10 min and left at room temperature to evaporate under an argon stream. Pale yellow crystals were separated one week later. Yield approximately 70%. Elemental analysis (%) calcd for $C_8H_8N_6Au_2O_2Fe$: C 14.34, H 1.20, N 12.54; found: C 14.95, H 1.50, N 12.03.

2Ag and **2Au**: Dehydrated samples **2Ag** and **2Au** were prepared from **1Ag** and **1Au** in the SQUID sample holder. Hydrated samples placed in sealed containers in the SQUID sample holder and their magnetism checked. Small holes were then made in the lids of the sample containers and the samples left standing for 30 min at 380 K, dehydration under these conditions is confirmed by the thermogravimetric analysis (see Supporting Information).

Received: May 9, 2003 [Z51853]
Published online: July 28, 2003

Keywords: allosterism · cooperative effects · crystalline-state reactions · N ligands · spin crossover

[1] a) J. M. Lehn, *Science* **2002**, *295*, 2400; b) M. D. Hollingsworth, *Science* **2002**, *295*, 2410.

[2] P. Gütlich, A. Hauser, H. Spiering, *Angew. Chem.* **1994**, *106*, 2109; *Angew. Chem. Int. Ed. Engl.* **1994**, *33*, 2024.

[3] J. A. Real, A. B. Gaspar, V. Niel, M. C. Muñoz, *Coord. Chem. Rev.* **2003**, *236*, 121.

[4] W. Vreugdenhill, J. H. Van Diemen, R. A. G. De Graaff, J. G. Haasnoot, J. Reedijk, A. M. Van der Kraan, O. Kahn, J. Zarembowitch, *Polyhedron* **1990**, *9*, 2971.

[5] O. Kahn, C. J. Martinez, *Science* **1998**, *279*, 44.

[6] T. Iwamoto in *Inclusion Compounds, Vol. 5* (Eds.: J. L. Atwood, J. E. D. Davies, D. D. MacNicol), Oxford University Press, London, UK, **1991**, p. 177.

[7] T. Kitazawa, Y. Gomi, M. Takahashi, M. Takeda, A. Enemoto, T. Miyazaki, T. Enoki, *J. Mater. Chem.* **1996**, *6*, 119.

[8] V. Niel, J. M. Martinez-Agudo, M. C. Muñoz, A. B. Gaspar, J. A. Real, *Inorg. Chem.* **2001**, *40*, 3838.

[9] V. Niel, M. C. Muñoz, A. B. Gaspar, A. Galet, G. Levchenko, J. A. Real, *Chem. Eur. J.* **2002**, *8*, 2446.

[10] V. Niel, A. Galet, A. B. Gaspar, M. C. Muñoz, J. A. Real, *Chem. Commun.* **2003**, 1248.

[11] a) B. Chen, M. Eddaoudi, S. T. Hyde, M. O'Keeffe, O. M. Yaghi, *Science* **2001**, *291*, 1021; b) O. M. Yaghi, G. Li, H. Li, *Nature* **1995**, *378*, 703.

[12] P. J. Langley, J. Hulliguer, *Chem. Soc. Rev.* **1999**, *28*, 279.

[13] a) G. J. Halder, C. J. Kepert, B. Moubaraki, K. S. Murray, J. D. Cashion, *Science* **2002**, *298*, 1762; b) J. A. Real, E. Andrés, M. C. Muñoz, M. Julve, T. Granier, A. Bousseksou, F. Varret, *Science* **1995**, *268*, 265.

[14] M. Albrecht, M. Lutz, A. L. Spek, G. van Koten, *Nature* **2000**, *406*, 970.

[15] Crystal for **1Ag**: Monoclinic, space group $P2_1/c$, $a = 14.7035(5)$, $b = 13.2962(5)$, $c = 7.3852(3)$ Å, $\beta = 91.441(2)°$, $Z = 4$, $V = 1443.35(9)$ Å^3, $T = 225$ K, $\rho_{calcd} = 2.263$ mg m^{-3}, $\mu = 3.683$ mm^{-1}, 19016 reflections measured, 3867 unique ($R_{int} = 0.0245$) which were used in all calculations and 3425 greater than $2\sigma(I)$. The final $R(F)$ was 0.0219 ($I > 2\sigma(I)$ data) and the $wR(F^2)$ was 0.0535 (all data). Crystal data for **1Au**: Monoclinic, space group $P2_1/c$, $a = 14.6157(5)$, $b = 13.3075(5)$, $c = 7.2272(3)$ Å, $\beta = 90.944(2)°$, $V = 1405.49(9)$ Å^3, $\rho_{calcd} = 3.166$ mg m^{-3}, $T = 180$ K, $\mu = 21.849$ mm^{-1}, 15805 reflections measured, 3072 unique ($R_{int} = 0.0545$) which were used in all calculations and 2441 greater than $2\sigma(I)$. The final $R(F)$ was 0.0241 ($I > 2\sigma(I)$ data) and the $wR(F^2)$ was 0.0474 (all data). CCDC-209792–209795 contain the supplementary crystallographic data for this paper. These data can be obtained free of charge via www.ccdc.cam.ac.uk/conts/retrieving.html (or from the Cambridge Crystallographic Data Centre, 12 Union Road, Cambridge CB2 1EZ, UK; fax: (+44) 1223-336-033; or deposit@ccdc.cam.ac.uk).

[16] L. Carlucci, G. Ciani, P. Macchi, D. M. Proserpio, *Chem. Commun.* **1998**, 1837.

[17] M. O'Keeffe, M. Eddaoudi, H. Li, T. Reineke, O. M. Yaghi, *J. Solid State Chem.* **2000**, *152*, 3.

[18] Crystal data for **2Au**: Monoclinic, space group $P2_1/c$, $a = 12.3855(7)$, $b = 13.6751(6)$, $c = 8.3348(4)$ Å, $\beta = 94.150(3)°$, $V = 1407.98(15)$ Å^3, $Z = 4$, $T = 293$ K. Final $wR_p = 7.46\%$, $R_F = 5.15\%$, GooF = 2.61, $\chi^2 = 6.827$ (see Supporting Information for structure refinement).

[19] J. D. Ranford, J. J. Vittal, D. Wu, *Angew. Chem.* **1998**, *110*, 1159; *Angew. Chem. Int. Ed.* **1998**, *37*, 1114.

 DOI: 10.1002/ange.200351246